Thomas, G. J., Jr. (1985) *Spectrochim. Acta 41A*, 217-221.
Thomas, G. J., Jr. (1987) in *Biological Applications of Raman Spectroscopy* (Spiro, T. G., Ed.) Vol. 1, pp 135-201, Wiley, New York.
Thomas, G. J., Jr., & Hartman, K. A. (1973) *Biochim. Biophys. Acta 312*, 311-322.
Thomas, G. J., Jr., & Agard, D. A. (1984) *Biophys. J. 46*, 763-768.
Thomas, G. J., Jr., & Benevides, J. M. (1985) *Biopolymers 24*, 1101-1105.
Thomas, G. J., Jr., & Wang, A. H.-J. (1988) in *Nucleic Acids and Molecular Biology* (Eckstein, F., & Lilley, D. M. J., Eds.) Vol. 2, pp 1-30, Springer-Verlag, Berlin.
Thomas, G. J., Jr., Li, Y., Fuller, M. T., & King, J. (1982) *Biochemistry 21*, 3866-3878.
Thomas, G. J., Jr., Benevides, J. M., & Prescott, B. (1986a) *Biomol. Stereodyn. 4*, 227-254.
Thomas, G. J., Jr., Prescott, B., Benevides, J. M., & Weiss, M. A. (1986b) *Biochemistry 25*, 6768-6778.
Tomlinson, B. L., & Peticolas, W. L. (1970) *J. Chem. Phys. 52*, 2154-2156.
Verduin, B. J. M., Prescott, B., & Thomas, G. J., Jr. (1984) *Biochemistry 23*, 4301-4308.
Webster, R. E., Grant, R. A., & Hamilton, L. A. W. (1981) *J. Mol. Biol. 152*, 357-374.
Wells, R. D., Goodman, T. C., Hillen, W., Horn, G. T., Klein, R. D., Larson, J. E., Muller, U. R., Neuendorf, S. K., Panayotatos, N., & Stirdivant, S. M. (1980) *Prog. Nucleic Acids Res. Mol. Biol. 24*, 167-267.
Willingmann, P., Krishnaswamy, S., McKenna, R., Smith, T. J., Olson, N. H., Rossmann, M. G., Stow, P. L., & Incardona, N. L. (1990) *J. Mol. Biol. 212*, 345-350.

Removal of DNA Curving by DNA Ligands: Gel Electrophoresis Study†

Francisca Barcelo,‡,§ Gabriel Muzard,‡,∥ Roberto Mendoza,‡ Bernard Rêvet,‡ Bernard Pierre Roques,⊥ and Jean-Bernard Le Pecq*,‡

Unitê de Physicochimie Macromolêculaire et Laboratoire de Microscopie Cellulaire et Molêculaire, INSERM U140, CNRS URA147, Institut Gustave-Roussy, 94805 Villejuif Cedex, France, and Dêpartement de Chimie Organique, INSERM U266, CNRS URA498, UER des Sciences Pharmaceutiques et Biologiques, 4 Avenue de l'Observatoire, 75006 Paris, France

Received November 7, 1990; Revised Manuscript Received February 8, 1991

ABSTRACT: The removal of inherent curving in *Crithidia fasciculata* kinetoplast DNA by various small DNA ligands, groove binders and mono- and bisintercalators, has been studied by gel retardation and electron microscopy. The migration of the kinetoplast DNA fragment is highly retarded during gel electrophoresis. We demonstrate that this retardation is suppressed by DNA ligands such as distamycin and ditercalinium, which have different modes of binding and sequence specificities. Observation by electron microscopy confirms that the effect of ditercalinium on gel migration of curved DNA is linked to DNA uncurving. As the drug is progressively added to DNA, a large broadening of the retarded band is observed during gel electrophoresis for distamycin and ditercalinium. In the case of distamycin, the retarded DNA band splits into two broad bands, whereas the noncurved DNA bands remain homogeneous. This indicates that the drug–DNA exchange is extremely slow in the gel and that a limited number of specific sites on DNA are critical for the removal of bending. GC-specific quinomycin, monointercalators, and bisintercalators act in a manner similar to that of AT-specific distamycin. This indicates that direct drug binding at the dA_n tracts is not required for DNA uncurving. We propose that the uncurving of kinetoplast DNA by drugs is caused by a global alteration of DNA structure; subsequent increased flexibility leads to the suppression of rigid bending at the AT tract junctions.

DNA sequences such as enhancers control the activity of promoters located at a distance on the DNA molecule. It has been shown that such remote control involves the interaction of proteins bound at distant sites on DNA through the formation of DNA loops. The implication of DNA looping in various biological processes has recently been discussed (Schleif, 1988). The formation of such DNA loops is limited by the bending ability of DNA (Wang & Giaever, 1988).

Therefore, inherently curved DNA sequences (Trifonov & Ulanovsky, 1988) would favor the interaction of proteins bound at distant sites on DNA by decreasing the free energy of loop formation. In this context, knowing whether small ligands such as antibiotics or antitumor drugs are able to remove or induce DNA curvature is of crucial importance.

Gel electrophoresis is a very powerful technique for the analysis of DNA bending. It demonstrated that pyrimidine dimers and covalent adducts such as GG intrastrand cisplatinum adducts induce DNA bending (Rice et al., 1988). On the other hand, the photoactivated covalent fixation of trimethylpsoralen on DNA was not found to produce significant bending (Sinden & Hagerman, 1984; Haran & Crothers, 1988).

Gel electrophoresis has also been used to analyze the effect of the reversible binding of proteins on DNA. No dissociation has been observed during gel migration because of the highly stable complexes. Therefore, the reversible complex could be analyzed in the same way as a covalent adduct. However, this method, which is appropriate for protein–DNA complexes, is not expected to be suitable for the study of the DNA bending induced by ligands that have a relatively small DNA binding

† This work was supported by INSERM, Contrat de Recherche 862009.
* To whom correspondence should be addressed.
‡ Institut Gustave-Roussy.
§ Present address: University les Iles Balears, Department of Biology, Faculty of Sciences, 07071 Palma of Mallorca, Spain.
∥ Present address: Laboratoire Theramex, BP 59, Monaco.
⊥ UER des Sciences Pharmaceutiques et Biologiques.

0006-2960/91/0430-4863$02.50/0

Table I: Physicochemical Properties of the Compounds Studied[a]

		charge (+) (pH = 8)	n	K_a (μM^{-1}) thymus	change of winding angle	sequence specificity[b]	reference
compound **1a** $(CH_2)_m$							
m = 0 (ditercalinium)	BI	2	5	10	−20		
1	BI	2	5	100	−24		
2	BI	2	5	70	−26		
3	BI	2	5	50	−29		
0 N^7-CH_3	BI	2	5	20	−52		
compound **1b**		4	4	50	−29		
ethidium dimer	BI*	4	5.5	200	−26		
quinomycin C	BI	0	5.5	3	−48	CG	1
ethidium bromide	MI*	1	2.2	1	−26	Py-Pu	2
actinomycin	MI	0	6.6	1	−26	GC (GG and CC)	3
N^2-methylellipticinium	MI*	1	2.5		−13		
N^2,N^6-dimethyl-9-hydroxyellipticinium	MI	1	2.5	5	−15		
N^2-ethylpiperidino-9-hydroxyellipticinium	MI	1	2.5	10	−14		
chromomycin	GB	0			+4	GGG, AGC (Mg)	4
distamycin	GB	1	5	10–100	+2	AT	3
netropsin	GB	2	4			AT	5
Hoechst 33258	GB*	1	4			AT	6

[a] BI = bisintercalator; MI = monointercalator; GB = groove binder. Fluorescent compounds are indicated with an asterisk; n = approximate number of base pairs covered by the DNA ligand. Winding angles were determined by the band counting method (Keller, 1975). Calf thymus DNA binding affinities were measured in 0.1 M NaCl/10 mM Tris-HCl buffer, pH 7, at 20 °C. [b] Sequence specificities have been taken from the following references: (1) Van Dyke and Dervan (1984); (2) Waring (1981); (3) Fox and Waring (1984); (4) Van Dyke and Dervan (1983); (5) Van Dyke et al. (1982); (6) Zimmer and Wahnert (1986).

constant. In that case, the DNA complex is expected to dissociate during gel electrophoresis. Nevertheless, distamycin (Wu & Crothers, 1984) and oligoacridines (Nielsen et al., 1988) have been shown to comigrate with DNA during gel electrophoresis. These experiments revealed that, contrary to expectation, these positively charged DNA ligands, whose residence occupancy times on DNA in solution are much smaller than their electrophoretic times, do not dissociate significantly from DNA during electrophoresis. To determine to what extent DNA uncurving by small ligands could be studied by gel electrophoresis, it was first necessary to control the comigration of various ligands of interest with DNA and determine the conditions under which such comigration is observed.

In order to determine the alteration of DNA curving by DNA ligands, we studied the specific retardation in gel electrophoresis of inherently curved kinetoplast DNA. We used the pPK201/CAT plasmid, which is a construction from pSP65 with the insertion of a 211-bp curved kinetoplast sequence from *Crithidia fasciculata* (Kitchin et al., 1986). This sequence contains 18 runs of 4–6 A's, 16 of which are located on the same strand (Kitchin et al., 1986). This periodic succession of dA_n tracts is at the origin of DNA curvature (Trifonov & Sussman, 1980; Marini et al., 1982; Hagerman, 1985; Koo et al., 1986). The periodical distribution of these dA_n tracts runs exactly in phase with the DNA helical pitch (10.5 bp; Mendoza et al., 1990). A curved kinetoplast DNA fragment has been directly observed by electron microscopy (Griffith et al., 1986; Thêveny et al., 1988). The drugs studied in this paper have been chosen among minor groove binders and mono- and bisintercalators.

Materials and Methods

Drugs and DNA. The synthesis of ditercalinium and its derivatives has been reported previously (Pelaprat et al., 1980). Ethidium dimer was synthesized as described (Roques et al., 1976). Ellipticine derivatives were prepared in our laboratory by Dr. E. Lescot. The structures of ditercalinium and ellipticine derivatives are presented in Figure 1. Distamycin was purchased from Sigma and actinomycin D (dactinomycin) from Merck. Hoechst 33258 was from Hoechst company.

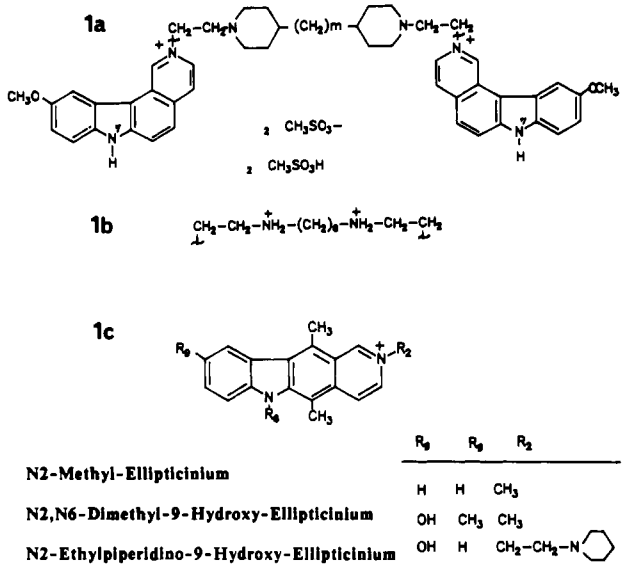

FIGURE 1: Structures of the pyridocarbazole compounds studied: (**1a** and **1b**) ditercalinium derivatives (m is the number of methylenes between the piperidine rings, 0, 1, 2, or 3); (**1c**) ellipticinium derivatives.

Netropsin was a gift from Dr. C. Auclair, chromomycin A3 was from Dr. R. H. Shafer (University of California, San Francisco) and quinomycin C (RP 50186) was from Dr. F. Lavelle (Rhône-Poulenc Santé, Vitry, France). Stock solutions were freshly prepared in water. Due to its low aqueous solubility, quinomycin C was prepared in methanol buffer (40/60 v/v) so that the final concentration of methanol in the reaction mixture was lower than 6%. A summary of the main physicochemical properties of these compounds is presented in Table I.

The plasmid DNA pPK201/CAT containing the 211-bp curved DNA fragment from the *C. fasciculata* kinetoplast fragment (Kitchin et al., 1986) was kindly provided by Dr. Paul T. Englund (Department of Biological Chemistry, The Johns Hopkins University School of Medicine, Baltimore, MD). Poly(dA)·poly(dT), poly(dA-dT)·poly(dA-dT), and calf thymus DNA were purchased from Boehringer Mannheim. The 123-bp DNA ladder is a set of n-mers of a 123-bp se-

quence (Hartley & Gregory, 1981) and was obtained from GIBCO BRL (Cergy-Pontoise, France).

pPK 201/CAT Enzyme Digestion. The plasmid (15 μg in 200 μL) was incubated with *Eco*RI (8 units), *Hin*dIII (2 units), and *Ava*II (6 units) for 2 h at 37 °C in (high ionic strength buffer) 50 mM Tris/10 mM $MgCl_2$/100 mM NaCl/1 mM dithioerythritol, pH 8 (Boehringer Mannheim). The incubation was stopped at 0 °C with 10 mM Na_2EDTA. Digestion was checked by electrophoresis on agarose gel. The DNA was purified by phenol and chloroform/isoamyl alcohol extractions and ethanol precipitation and then redissolved in 10 mM Tris/1 mM EDTA, pH 8 (TE buffer) at a final concentration of 100 μg/mL (Maniatis et al., 1982).

Digestion of the plasmid pPK201/CAT (3228 bp) by the restriction enzymes *Eco*RI, *Hin*dIII, and *Ava*II gave four DNA fragment sizes: 219, 264, 1345, and 1386 bp. The 264-bp fragment contains the 211-bp curved *C. fasciculata* kinetoplast DNA sequence. Digestion of pPK201/CAT by *Hin*fI alone was performed in the same experimental conditions and yielded eight fragments (65, 75, 211, 354, 396, 412, 517, and 1198 bp). The 412-bp fragment contained the curved kinetoplast sequence (211 bp) between bases 184 and 394.

Gel Electrophoresis of Drug–DNA Fragment Complexes. Reaction mixtures (typically 10 μL) of drug–DNA complexes were done in TE buffer with 70 μM DNA (in bp) and with increasing drug concentrations (rf = 0–0.3). Formal rf values are defined as total molar drug concentration relative to the total DNA concentration expressed in base pairs. After incubation at room temperature for 1 h, 5 μL of loading buffer (5% glycerol/0.04% bromophenol blue) was added. The samples were then loaded onto a 5% polyacrylamide gel in TBE buffer (0.1 M Tris base/0.1 M boric acid/1 mM EDTA, pH 8) and subjected to electrophoresis at 5 V/cm for 5 h, or at 2 V/cm overnight in the dark, at 4 °C. Gels were subjected to preelectrophoresis for 2 h before sample application. Gels were stained with ethidium bromide (0.5 μg/mL) during 30 min and then exhaustively washed and photographed under UV light through a red filter. In the case of complexes between fluorescent drugs and DNA fragments, gels were visualized directly without ethidium staining and photographed under UV light through a yellow filter.

The 123-bp DNA ladder has been taken as a standard to relate gel migrations to apparent fragment sizes. For each gel, the size of the *n*-mers has been plotted as a function of the distance of electrophoretic migration. Data were then fitted to a polynomial function. The apparent size (RL) of the pPK201/CAT fragments was calculated from the electrophoretic migration distances by interpolation with use of the previously determined polynomial function.

Gel Electrophoresis of DNA in the Presence of Two Competing Drugs. DNA fragments (70 μM) were incubated at room temperature for 1 h with either distamycin (rf = 0.064), actinomycin D (rf = 0.107), quinomycin C (rf = 0.15), or chromomycin A_3 (rf = 0.15). Distamycin or ditercalinium was then added as a competing drug with rf values from 0/bp to 0.15/bp to aliquots (10 μL) of each incubation mixture. After 1 h of equilibration, loading buffer was added and the samples were electrophoresed as described above. Complexes between native DNA fragments and competing drugs alone were incubated at the same rf values under the same experimental conditions and used as controls.

Binding Studies. Binding of ethidium dimer to poly(dA)·poly(dT) and poly(dA-dT)·poly(dA-dT) was determined by direct fluorometric titration in 0.1 M Tris-HCl/0.1M NaCl, pH 7.4, at room temperature as has been previously described for calf thymus DNA (Gaugain et al., 1978). Binding of ditercalinium to poly(dA)·poly(dT), poly(dA-dT)·poly(dA-dT), and calf thymus DNA was determined by direct absorbance titration at room temperature with a Uvikon 861 spectrophotometer equipped with semicompartment cuvettes (1- or 5-cm path length). Saturation curves were drawn from absorbance variations at 258 or 320 nm and directly fitted with the neighbor-exclusion model (McGhee & von Hippel, 1974).

Untwisting of the DNA helix induced by distamycin or chromomycin A_3 was measured by the change in electrophoretic migration in agarose gel of the supercoiled plasmid pUC13 DNA incubated with those ligands as described (Garbay-Jaureguiberry et al., 1987).

Electron Microscopy Measurements. The 264-bp pPK201/CAT restriction fragment containing the curved DNA was purified by FPLC chromatography on a MonoQ column (Pharmacia) with a Tris/NaCl gradient (Tris 0.1 M, pH 7.4; NaCl 0.4–1 M). A total of 10 μL of the isolated fragment at a final DNA concentration of 1 μg/mL was incubated with varying concentrations of ditercalinium or ethidium monomer at 4 °C for 1 h. The complexes formed were deposited at 4 °C on carbon grids to be observed in a Zeiss 902 electron microscope. Images of 50 molecules were digitized for each ligand–DNA complex (Joanicot & Rêvet, 1987; Thêveny et al., 1988; Muzard et al., 1990). The contour length of each DNA molecule was determined. The curvilinear length of each molecule in the absence (L_0) and in the presence of drug (L) and the linear end-to-end length (D) was measured for each drug concentration. The mean values and standard errors of L and L/D were calculated.

Results

Use of Gel Retardation To Study Reversible Ligand–DNA Interactions. Before analyzing reversible DNA complexes by gel electrophoresis, it was first necessary to check that dissociation was negligible during electrophoresis. We therefore studied the migration of DNA complexes using fluorescent DNA ligands (Table I) with different affinity constants ranging from 10^5 to 10^8 M^{-1}. Complexes were preformed by incubation with *Hin*fI pPK201/CAT fragments or with *n*-mers of the 123-bp DNA ladder. After gel migration, the fluorescence of the DNA fragments was directly quantified before gel staining and normalized for the length of the fragments (Figure 2). This normalized fluorescence represents the quantity of the ligand that migrates per unit of DNA length. Ethidium dimer is a bisintercalating agent with two quaternary ammonium positive charges and a high DNA affinity constant (10^8 M^{-1}) (Roques et al., 1976). Ethidium dimer clearly comigrates with all DNA fragments (Figure 2A). Moreover, it causes considerable retardation of all fragments except for the curved fragment, as will be discussed later. Ethidium monomer and N^2-methylellipticinium are monointercalating agents with one positive charge. They have much lower DNA binding affinities than the ethidium dimer (Table I) (Roques et al., 1976). The comigration of these compounds with the 354-bp fragment and with larger sized fragments is clearly detected by fluorescence but is not observed for the smallest fragment (211 bp). Ethidium monomer modifies DNA fragment mobility. Comigration with 517- and 1198-bp fragments is observed for N^2-methylellipticinium without any modification of electrophoretic mobility. The fluorescence of each DNA restriction fragment normalized to fragment size, which represents the amount of drug per unit of DNA length, has been plotted according to the amount of N^2-methylellipticinium added (Figure 2D). Normalized fluorescence is proportional to the rf values. It is independent of the size of

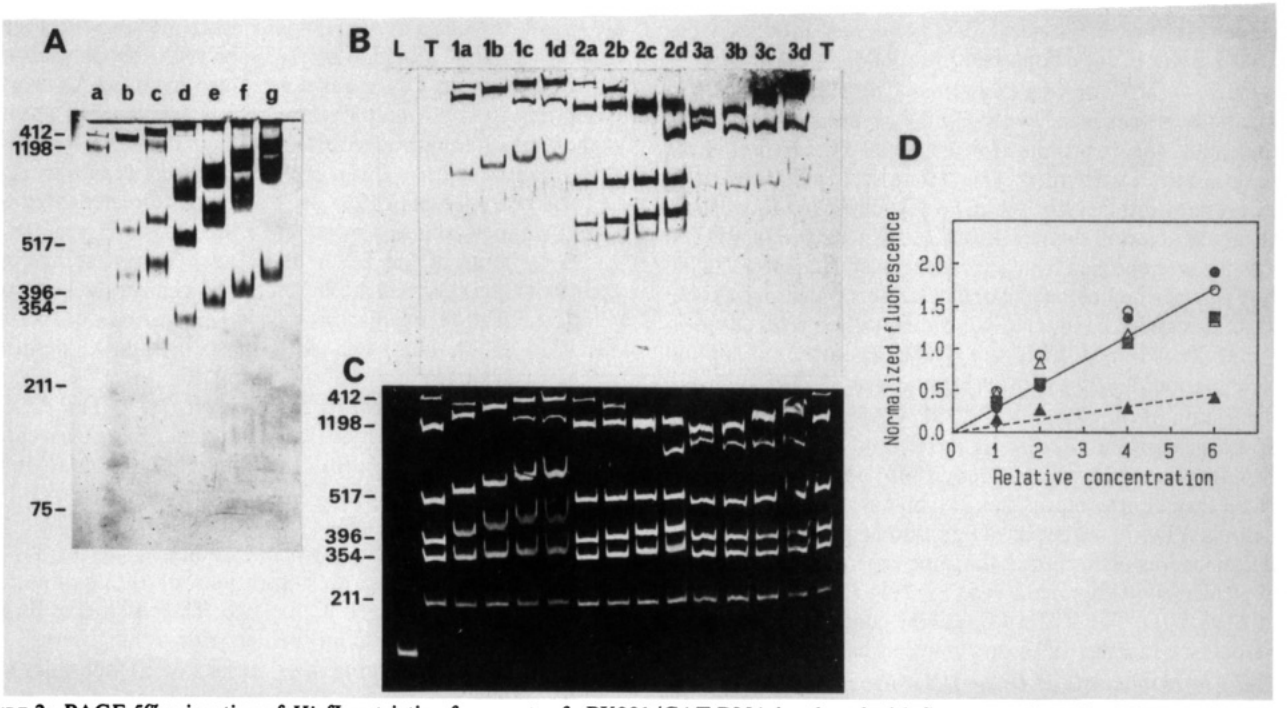

FIGURE 2: PAGE 5% migration of *Hin*fI restriction fragments of pPK201/CAT DNA incubated with fluorescent ligands. Gels A and B show direct fluorescence without staining. Gel A shows the ethidium dimer at rf values (a) 0.021, (b) 0.042, (c) 0.064, (d) 0.107, (e) 0.15, (f) 0.19, and (g) 0.24. Gel B shows (1) ethidium monomer, (2) N^2-methyllellipticinium, and (3) Hoechst 33258 at rf values (a) 0.07, (b) 0.14, (c) 0.28, and (d) 0.42. Lane L shows 123 *n*-mers DNA ladder; lane T shows DNA restriction fragments without drug. Gel C is gel B after ethidium staining. Panel D shows N^2-methyllellipticinium fluorescence normalized to fragment size for the restriction fragments of gel B (lanes 2a–2d) as a function of drug concentrations expressed in rf values (moles of drug added per moles of DNA in bp). The length of the fragment (in bp) is (▲) 354, (▲) 396, (■) 412, (○) 517, or (●) 1198.

the DNA restriction fragments for a given drug concentration except in the case of the smallest DNA fragment, which partially retains the drug. Hoechst 33258 is a fluorescent groove binder, with one positive charge at pH 8. Its fluorescence is negligible on fragments smaller than 396 bp but much higher on the curved 412-bp fragment than on the 517-bp fragment. This property might be explained by the strict specificity of this drug for AT-rich sequences (Zimmer & Wahnert, 1986).

With the 123-bp DNA ladder, it is possible to further extend the relationship between DNA fragment length and comigration of the drug with DNA. Ethidium dimer fluorescence is observed on all DNA fragments (Figure 3A) and qualitatively confirms that the ethidium dimer comigrates almost equally well with all bands but its fluorescence could not be directly quantified with precision because of a large smear on the bands. Ethidium monomer fluorescence was only observed on the longest DNA fragments (data not shown). These experiments distinctly show that comigration is dependent on both DNA length and the ligand binding constant. When the binding constant is greater than 10^6 M^{-1} and the length is greater than 354 base pairs, no significant dissociation of the complexes is observed during electrophoresis. Experimental conditions and ligands can now be selected that do not cause significant DNA–ligand complex dissociation during gel electrophoresis.

Effect of Ligand Binding on Uncurved DNA Migration. The *n*-mers of the DNA ladder complexed with the ethidium dimer or distamycin show retarded migrations (Figure 3A). The gel retardation of each band has been quantified in terms of apparent to true fragment size ratios (RL). For distamycin (Figure 3B), RL increases with ligand concentration (expressed in rf values) and reaches a plateau. At given distamycin concentrations, RL also increases with fragment length and a plateau is reached for a length of 1000 bp (Figure 3C). The same phenomenon is observed for ethidium dimer with a much higher amplitude (Figure 3A). Ditercalinium behavior is similar to that of distamycin and different from that of actinomycin D, which has been found to modify only slightly the gel migration of the *n*-mers. The migration of the longest fragments is only modified at high drug concentrations (data not shown). Thus, the gel retardation of the ligand–*n*-mer complexes depends on the drug and on the length of the DNA fragment. Maximum RL values observed for the migration of the 123 *n*-mers were plotted for each of the compounds studied (Figure 3D).

The reversibility of the ligand inducing gel retardation effects was controlled. Complexes between ligands and DNA restriction fragments were incubated in the presence of 1% SDS or treated with ethanol before loading onto the gel. Gel mobilities were found to be identical with those of DNA fragments alone. This demonstrates that the change in the electrophoretic mobility of the ligand–DNA complexes is a reversible process and is not associated with the formation of covalent adducts during preincubation time.

Curving Removal of the Kinetoplast DNA by Distamycin and Ditercalinium. Gel migration of *Eco*RI–*Hin*dIII–*Ava*II pPK201/CAT DNA restriction fragments was compared to that of the 123-bp DNA ladder *n*-mers (Figure 4A; lanes 0 and L). The 264-bp fragment, which contains the curved kinetoplast sequence, was dramatically retarded and migrated with the mobility of a 1150-bp fragment. Anomalous gel migration of DNA fragments was quantified by ratios of apparent RL to true fragment sizes according to Koo and Crothers (1988). Under our experimental conditions, RL = 4.35 for the 264-bp fragment. The 219-, 1345-, and 1386-bp fragments had RL = 0.9, 1.2, and 1.2, respectively. The 219-bp fragment is the 3510–3728 bp sequence from pBR322 and it is known not to be curved (Stellwagen, 1983; Muzard et al., 1990).

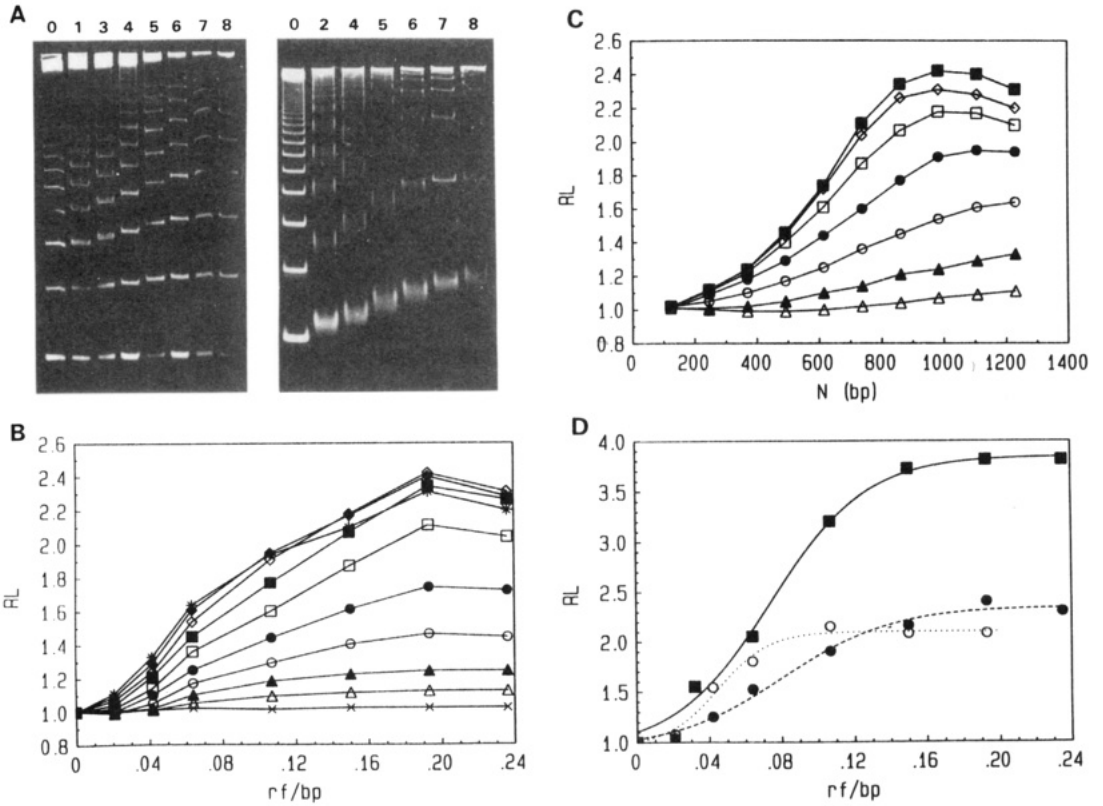

FIGURE 3: (A) PAGE 5% migration of the 123 DNA ladder with distamycin (left side) and ethidium dimer (right side) at rf values (0) 0, (1) 0.021, (2) 0.032, (3) 0.042, (4) 0.064, (5) 0.107, (6) 0.15, (7) 0.193, and (8) 0.24. Panels B–C show the relative migration of the 123 *n*-mers in the presence of distamycin. (B) RL plot as a function of the ligand concentration: *n*-mers are (×) 123, (△) 246, (▲) 369, (○) 492, (●) 615, (□) 738, (■) 861, (◇) 984, (◆) 1107, and (*) 1230. (C) RL plot as a function of the fragment size: the distamycin concentrations are (△) 0.021, (▲) 0.042, (○) 0.064, (●) 0.107, (□) 0.15, (◇) 0.183, and (■) 0.24. (D) Maximum RL values obtained for the migration of the 123 *n*-mers in the presence of (■) ethidium dimer, (●) ditercalinium, or (○) distamycin. RL is the ratio of the apparent to true size of a given DNA fragment.

The effect of distamycin on the gel migration of the pPK201/CAT fragments (Figure 4A) has been plotted in terms of RL ratios (Figure 4C). The three "normal" fragments (219, 1345, and 1386 bp) have reduced mobilities with increasing concentrations of distamycin. The gel retardation of the 264-bp fragment is considerably decreased but not completely removed (RL = 1.7) at distamycin saturating concentration when one distamycin molecule is bound per dA_n tract in the kinetoplast DNA. These results are in agreement with those obtained with the *Leishmania tarentolae* kinetoplast fragment (Wu & Crothers, 1984).

The effect of ditercalinium on the gel migration of the pPK201/CAT fragments has been studied in the same conditions and appears to be significantly different from that of distamycin (Figure 4B,D). Ditercalinium strongly reduces the mobility of the smallest 219-bp fragment. The migration of the 264-bp curved fragment does not seem to be affected at small ditercalinium concentrations, but its migration becomes identical with that of uncurved fragments at ligand saturation (RL = 1.4). Therefore, ditercalinium completely uncurves the kinetoplast fragment. No recurving was subsequently observed even at very high concentrations.

A large smear is observed for the 264-bp fragment migration at half-titration. In the case of distamycin, two peaks can be resolved (Figure 4E) under similar conditions. This indicates that an exchange does not occur between the drug and its binding site during electrophoresis, as will be discussed later. A very large smear free of band splitting is observed with ditercalinium (Figure 4F).

In order to determine the ditercalinium binding specificity on AT-rich sequences and to relate it to the known distamycin specificity (Zimmer & Wahnert, 1986; Coll et al., 1987), we have measured binding affinities of this dimer on poly(dA)·poly(dT), poly(dA-dT)·poly(dA-dT), and calf thymus DNA. The affinity of ditercalinium for poly(dA-dT)·poly(dA-dT) is quite similar to that for calf thymus DNA (10^7 M^{-1}). We found that ditercalinium binds to poly(dA)·poly(dT) with a much lower affinity (5×10^5 M^{-1}) (data not shown). Under these conditions, ditercalinium is expected to interact preferentially with the non-dA_n tracts of the kinetoplast fragment, in agreement with DNase I footprinting studies (Mendoza et al., 1990).

Comparison of Kinetoplast DNA Uncurving by Various Other Ligands. Netropsin is a compound closely related to distamycin but with two positive charges and clear AT binding specificity (Zimmer & Wahnert, 1986). Netropsin appears to be less efficient than distamycin in removing the 264-bp fragment gel retardation (RL maximum = 2.4 instead of 1.7 for distamycin) (Figure 5A).

Ethidium dimer (Figure 5B) and quinomycin C (data not shown) are dimeric molecules that can be considered typical DNA bisintercalators (Wakelin, 1986). These two compounds show effects quite comparable to those elicited by ditercalinium on the gel mobility of the *Eco*RI–*Hin*dIII–*Ava*II pPK201/CAT DNA restriction fragments. This result shows that the number of charges on the ligand (4 for Ethidium dimer and none for quinomycin C) is not critical for DNA uncurving.

The ditercalinium derivatives (compounds **1a** with $m = 1$–3; Figure 1 and Table I) are bisintercalators characterized by an extension of the bis(piperidino) linking chain between the two pyridocarbazole chromophores. All these dimers bisintercalate into DNA but modify the DNA structure in a dif-

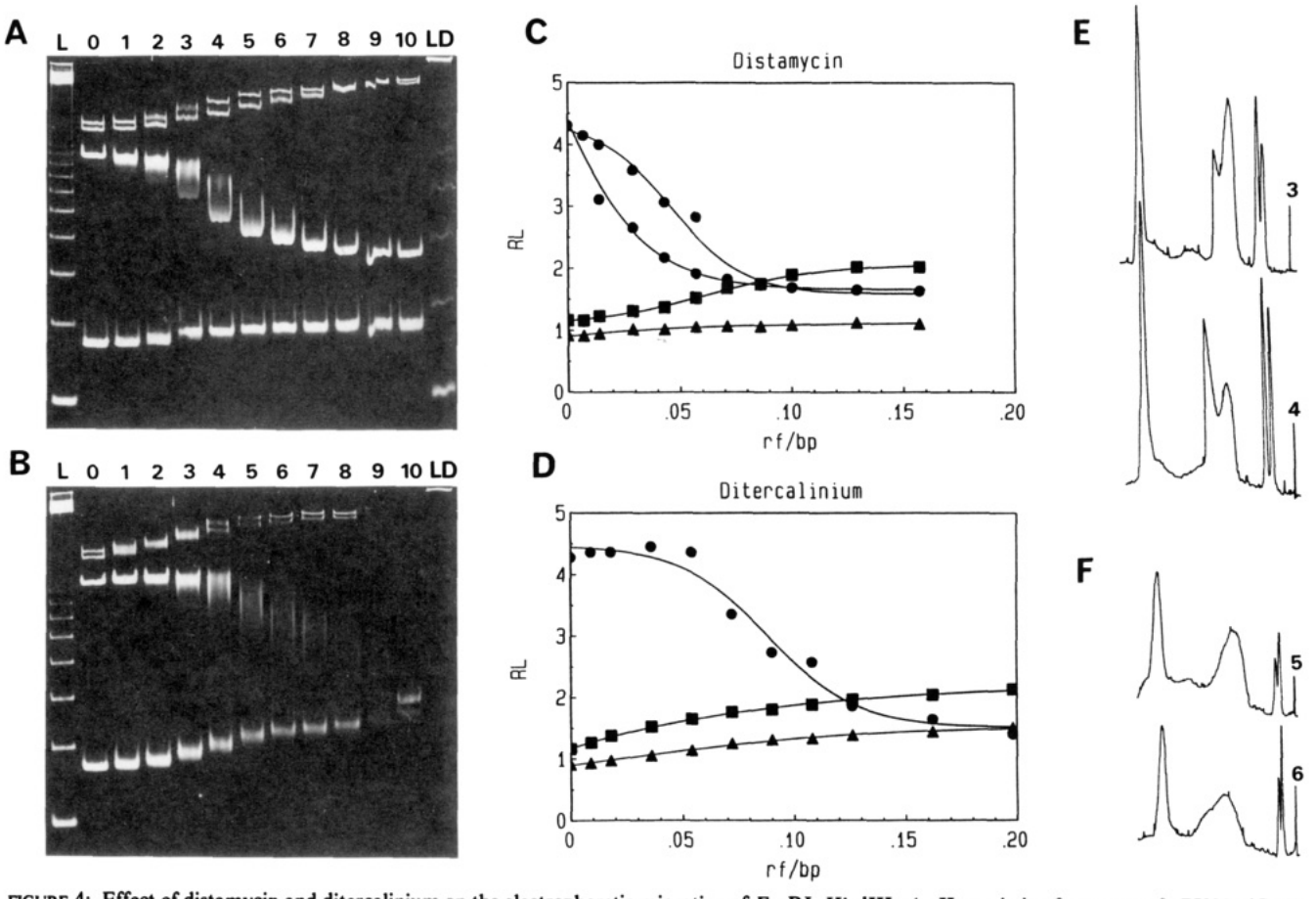

FIGURE 4: Effect of distamycin and ditercalinium on the electrophoretic migration of *Eco*RI–*Hin*dIII–*Ava*II restriction fragments of pPK201/CAT. The sizes of DNA fragments are 1386, 1345, 264 (curved DNA fragment), and 219 bp. (**A**) Lanes (1–10): distamycin at rf values 0.007, 0.014, 0.029, 0.043, 0.057, 0.071, 0.086, 0.1, 0.129, and 0.157. (**B**) Lanes (1–10): ditercalinium at rf values 0.009, 0.018, 0.036, 0.054, 0.072, 0.09, 0.108, 0.126, 0.162, and 0.198. Other lanes: (L) ladder; (0) DNA restriction fragments; (LD) ladder with distamycin or ditercalinium at rf 0.157 and rf 0.198, respectively. (**C–D**) RL plots of the fragments (△) 219, (●) 264, and (■) 1345 bp versus rf values. Solid lines are sigmoidal regression curves. (**E–F**) Densitometer scans of distamycin and ditercalinium at rf values 0.029 and 0.043 and rf values 0.072 and 0.09, respectively.

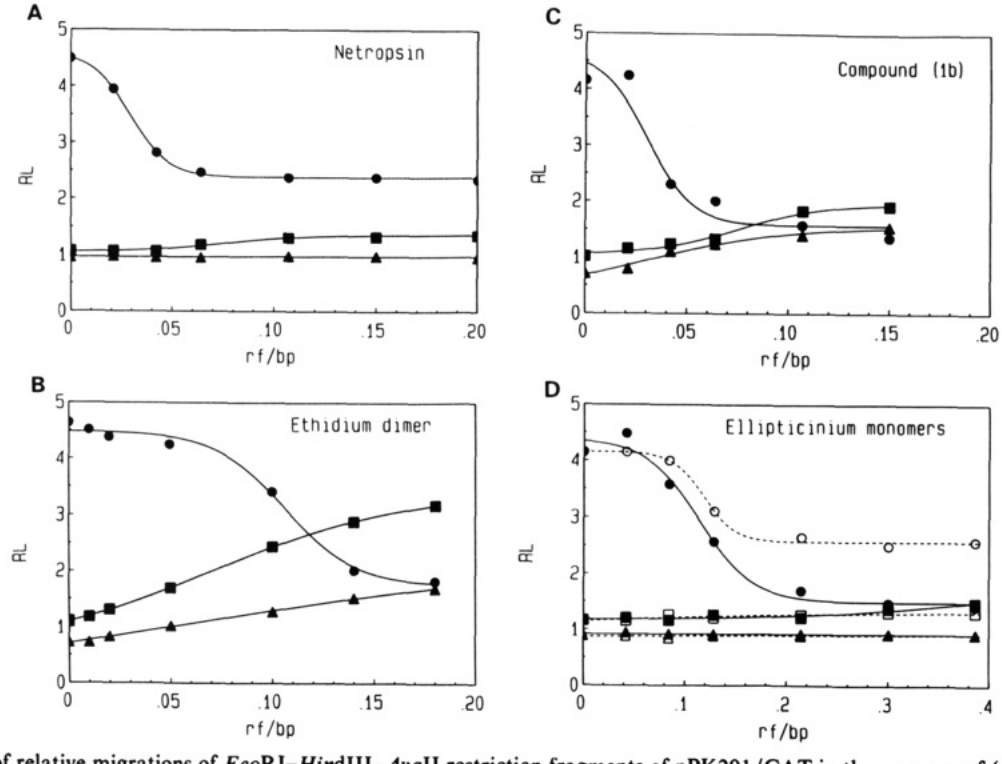

FIGURE 5: Plots of relative migrations of *Eco*RI–*Hin*dIII–*Ava*II restriction fragments of pPK201/CAT in the presence of (**A**) netropsin; (**B**) ethidium dimer; (**C**) compound 1b; (**D**) N^2,N^6-dimethyl-9-hydroxyellipticinium (closed symbols) and N^2-ethylpiperidino-9-hydroxyellipticinium (open symbols). DNA fragments are (▲) 219 bp, (●) 264 bp, and (■) 1345 bp. Solid lines are sigmoidal regression curves.

ferent manner (Garbay-Jaureguiberry et al., 1987). These derivatives show effects similar to those of ditercalinium on the gel migration of the pPK201/CAT fragments (data not shown). The ditercalinium derivative (**1a** with $m = 0$), which is derived from ditercalinium by substitution of methyl groups at the N^7 positions (Figure 1 and Table I), has a strikingly high DNA unwinding angle (−52°) compared to those of ditercalinium (−20°) and the other ditercalinium derivatives previously mentioned (Garbay-Jaureguiberry et al., 1987). However, the removal of the 264-bp fragment retardation is not different from that caused by ditercalinium. This result illustrates that ligand unwinding does not seem to be a significant parameter in the curving removal phenomenon. The ditercalinium bispiperidino linking chain for compound **1b** has been replaced by a spermine-like chain. This chain is highly flexible so that compound **1b** is expected to induce a smaller deformation of the helix axis than other derivatives. However, 264-bp fragment retardation is completely removed at even lower concentrations than with ditercalinium (Figure 5C).

The effects of related monomeric intercalating compounds (Figure 1) on the gel migration of the pPK201/CAT fragments could be studied by use of N^2,N^6-dimethyl-9-hydroxyellipticinium and N^2-ethylpiperidino-9-hydroxyellipticinium. These derivatives have high enough DNA binding affinities so that their DNA complexes are stable during gel migration. They have 1 net positive charge at pH 8 (Table I). Mobilities of the uncurved fragments are almost unaltered by these two compounds (Figure 5D). N^2,N^6-dimethyl-9-hydroxyellipticinium completely removes gel retardation of the curved fragment. The effect of the first derivative is equivalent to that of dimeric ligands. Contrastingly, N^2-ethylpiperidino-9-hydroxyellipticinium has a limited effect on the migration of this DNA fragment (RL maximum = 2.5).

Actinomycin D is an uncharged monointercalating DNA ligand (Muller & Crothers, 1968). As it is a GC-specific ligand, it is not supposed to interact with the dA_n tracts. Actinomycin D has no effect on the migration of the 219- and 264-bp fragments but does have a retarding effect on the 1345- and 1398-bp fragments (data not shown). Chromomycin A_3 is an uncharged nonintercalating DNA ligand that is specific to G-containing sequences (Van Dyke & Dervan, 1983). Chromomycin A3 induces only limited DNA conformational alterations exclusively in the presence of magnesium; we determined an unwinding angle of −4° by the band counting method (Table I), and we observed almost no effects on the gel migration of the pPK201/CAT fragments (data not shown).

As will be discussed later, some theories of DNA curving predict that two different ligands could add their effects in opposite ways on the curved fragment. Competition experiments between some sequence-specific ligands and ditercalinium should then provide information about the binding characteristics of the latter. *Eco*RI–*Hin*dIII–*Ava*II pPK201/CAT DNA restriction fragments were complexed with sequence-specific ligands at a constant rf value, and ditercalinium was subsequently added up to saturation. Experiments were done with distamycin (AT specific), quinomycin C (CG specific), and actinomycin D (GC specific). Ditercalinium produces additive effects on the migration of the 246-bp fragment in all cases (Figure 6). Similar results were obtained by adding distamycin to quinomycin C–DNA or actinomycin D–DNA complexes (data not shown).

Visualization by Electron Microscopy of DNA Uncurving. The effect of ligand binding on the 219- and 264-bp fragments has been directly investigated by electron microscopy analysis

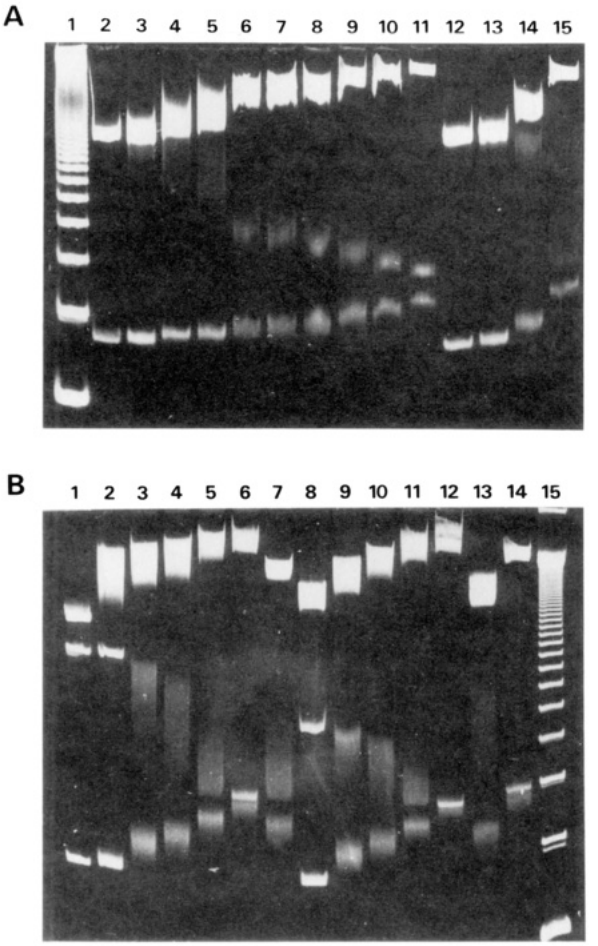

FIGURE 6: PAGE 5% migration of DNA–ligand complexes with competing ditercalinium. (**A**) DNA–quinomycin complexes: the lanes show (1) ladder; (2) *Eco*RI–*Hin*dIII–*Ava*II DNA restriction fragments; (3–6) DNA–quinomycin C complexes at rf values 0.042, 0.064, 0.107, and 0.15; (7–11) DNA–quinomycin C complex at rf 0.15 with competing ditercalinium at rf values 0.021, 0.042, 0.064, 0.107, and 0.15; (12–15) DNA–ditercalinium at rf values 0.011, 0.021, 0.042, and 0.107. (**B**) DNA–actinomycin and DNA–Distamycin complexes: the lanes show (1) DNA restriction fragments; (2–6) DNA–actinomycin complexes for rf 0.107 anmd competing ditercalinium at rf values 0, 0.042, 0.064, 0.107, and 0.15; (7) DNA–ditercalinium complexes at rf 0.107; (8–12) DNA–distamycin complexes at rf 0.064 and competing ditercalinium at rf values 0, 0.042, 0.064, 0.107, and 0.15; (13–14) DNA–ditercalinium complexes at rf values 0.064 and 0.15; (15) ladder.

for ditercalinium and ethidium monomer. The increase in the length (L) of the DNA fragment according to the amount of the ligand added has been shown to be a reliable measure of the true amount of ligand bound to the DNA in the case of intercalative drugs (Butour et al., 1978). The curvature of the DNA fragment is simply quantified by the ratio L/D of the contour length (L) to the linear end-to-end length (D) of the DNA molecule. This ratio is equal to 1 for a straight fragment and increases with the fragment curvature. The 219- and 264-bp fragments have L/D ratios equal to 1.25 and 3.8, respectively. The effect of ligand binding on the curvature of the fragments is given by the variations of L/D as a function of L/L_o (Figure 7). Ditercalinium removes the curving of the kinetoplast DNA fragment and the titration obtained is in agreement with the results obtained in gel electrophoresis (Figure 4D). Ethidium monomer, whose uncurving effect could not be seen by gel electrophoresis, also removes kinetoplast curving. The small increase of L/D for ditercalinium binding on the 219-bp fragment can be accounted for by the increase in length of this fragment as deduced from the data

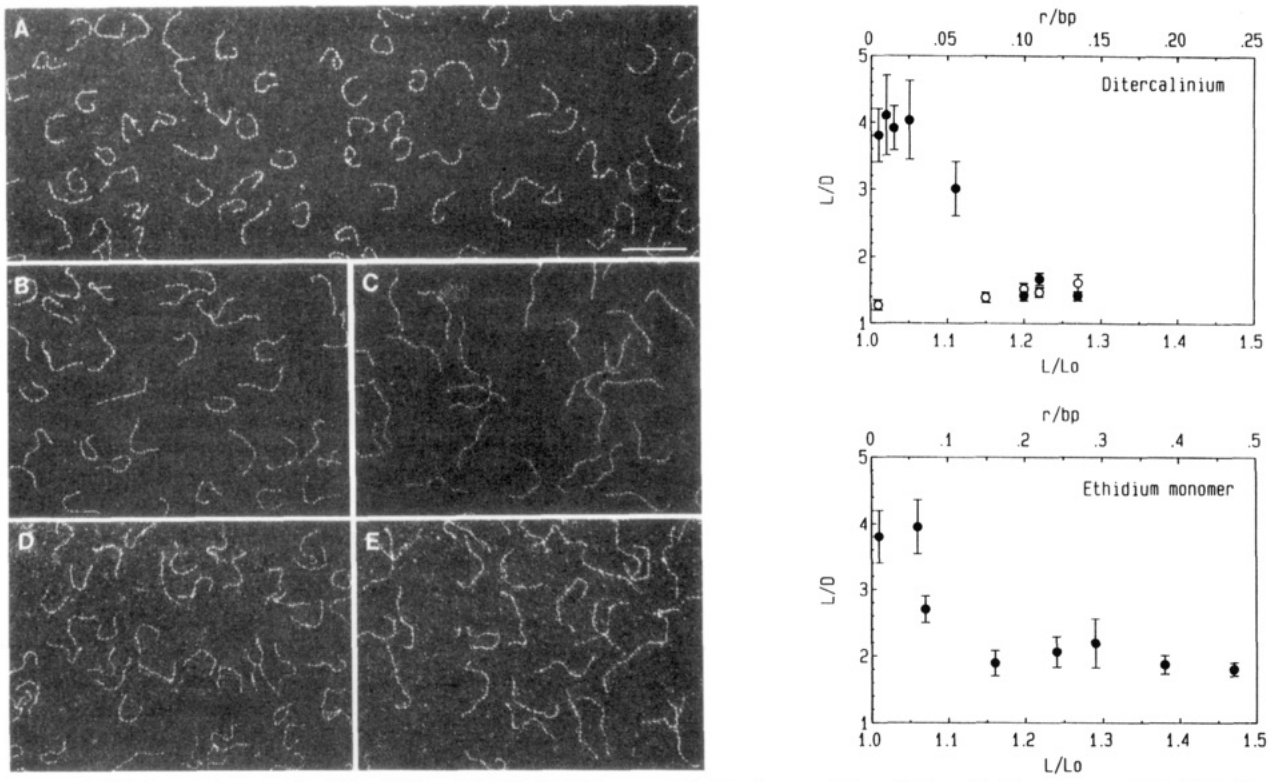

FIGURE 7: Electron migrographs of the 264-bp pPK201/CAT fragment in the absence of drug (A) and in the presence of the following drugs: ditercalinium at rf 0.05 (B) and 0.14 (C); ethidium monomer at rf 0.06 (D) and 0.47 (E). The graphs show ratios of the contour lengths to end-to-end distances (L/D) of the 264 (●) and 219 bp (○) pPK201/CAT fragments as a function of its length increase (L/L_0) for ditercalinium and ethidium monomer. Values have been obtained from the direct visualization by electron microscopy of 50 individual DNA molecules. The bar equals 0.01 μm.

of Joanicot and Rêvet (1987).

Discussion

Comigration of Ligands with DNA during Gel Electrophoresis. The gel retardation method was not expected to be suitable to study reversible DNA–ligand complexes in the case of compounds with positive charges and with low DNA affinities. Residence times of such ligands on DNA are in the millisecond–second range, while electrophoresis is performed during several hours. The migration of DNA in the electrophoretic field should favor the dissociation process especially in the case of positively charged ligands, which tend to migrate in a direction opposite to that of DNA.

Fluorescent compounds were used to demonstrate the comigration of ligands with DNA. Under our experimental conditions, it was observed that the ethidium dimer, which has a very high DNA affinity, comigrates with all DNA fragments from 75 to 1198 bp (Figure 2A), which is in agreement with Glazer et al. (1990). For other drugs, with lower affinities, comigrations were only observed with DNA fragments longer than a critical length. These critical lengths depend on the drugs. Figure 2B indicates that N^2-methylellipticinium comigrates with fragments above 354 bp, whereas ethidium and Hoechst 33258 comigrate only with fragments longer than 517 bp. It is therefore clear that both the length of DNA fragments and the binding affinity of the ligands are factors that critically influence the comigration of the ligands with DNA.

The absence of dissociation of DNA complexes that have a lifetime in the range of a millisecond–second during gel electrophoresis, which lasts several hours, have been observed with distamycin (Koo et al., 1986) and diacridines (Nielsen, 1988). Such observations have puzzled the experimentors, and several models have been proposed to account for such an apparently surprising fact. Nielsen et al. (1988) have proposed that the constrained structure of DNA fragments in the gel matrix favors a more effective reassociation process of dissociated ligands on DNA. It is argued that local concentrations of DNA and ligand are increased in the gel due to gel volume exclusion effects and that the structure of the gel gives rise to a "cage" effect that prevents ligand diffusion. Similar arguments have also been presented to explain comigration of reversible protein–DNA complexes (Fried & Crothers, 1981).

We have explored a simple model that just takes into account the dissociation of the complex while the DNA is migrating in the gel. The basis of such calculation is given in the appendix. Qualitatively, this model predicts the observed behavior of the dye–DNA complex during the gel electrophoresis, that is, almost no loss of dye at a high binding constant and complete loss at a low binding constant.

Furthermore, according to such a model, when several bands are comigrating in the gel, the faster band will load the gel with dye. At a given point, the concentration of the dye in the gel will be then the concentration that was at the passage of the fast moving band at equilibrium. This will prevent the dissociation in the slow migrating band and will explain the presence of a smear.

Gel Retardation of Ligand–DNA Complexes. We used the 123-bp DNA ladder to analyze the effect of DNA length on the rate of migration of ligand–DNA complexes. The advantage of using such a ladder is that only length effects are measured as the various fragments have the same base composition. For all ligands studied in this work, the rate of gel migration decreases with drug concentration. This corresponds to an apparent increase in DNA length (RL). When positively charged, the various ligands can neutralize the negative charge of DNA and slow down migration. However, this effect does not provide an explanation for the absence of retardation for

small fragments and the absence of a correlation between the number of charges neutralized by various ligands and the rate of migration. We believe that the main effect is on DNA conformation and flexibility.

In agreement with the present proposal it was recently reported that the DNA in the complex with ditercalinium is kinked by 15° and unwound by 36° with exceptionally wide major and minor grooves (Qi Gao et al., 1991).

Removal of DNA Curving. We show that compounds as different as distamycin and ditercalinium remove the retarded migration of the kinetoplast DNA fragment but not in the same way. Ditercalinium appears to be less efficient than distamycin in removing the retardation of the curved fragment at small concentrations but completely removes the retardation effect at a saturating concentration, which distamycin is unable to do. A large smear is observed during the uncurving of the 264-bp fragment with the two drugs. The appearance of two resolved peaks is observed for distamycin. Due to its AT specificity, distamycin will bind to a limited number of sites on the kinetoplast DNA fragment. Distamycin interaction on binding sites at the fragment ends is not expected to modify the gel migration of the DNA fragment (Wu & Crothers, 1984), whereas interaction on binding sites at the center of the curved DNA would remove gel retardation. Two families of drug distributions of DNA (more at the center or more at the ends) could then be obtained, leading to two migration peaks. These smears indicate that these compounds necessarily exchange slowly between binding sites during gel migration. If the occupancy of a very small number of sites located at the center of the DNA molecule is critical for the removal of bending, a large fluctuation in the occupancy of these sites at low drug concentration will cause a large fluctuation in the conformation of the different DNA molecules as it is observed. Furthermore, the appearance of two resolved distributions suggests that there is no exchange of ligand binding between the center and the periphery during the migration. This again underlines the absence of ligand dissociation during electrophoresis.

Ligand binding can lead to the removal of curving of the kinetoplast DNA fragment either by modifying the DNA helix twist and thus dephasing the curved tracts or by modifying dinucleotide wedges.

Possible Curving Removal by Dephasing. Distamycin induces very slight winding of the DNA helix (+2°) (Kopka et al., 1985). Dephasing is therefore negligible in that case. Ditercalinium DNA binding causes rather substantial unwinding of the DNA helix (−20°), which could in that case induce dephasing of the curved tracts. The contribution of ditercalinium to this unphasing within the removal of the 264-bp fragment curvature was estimated by the method of Muzard et al. (1990). About one ditercalinium molecule is bound for each half-turn of the non dA_n tracts at saturation. At this level, by taking into account only the unwinding effect of ditercalinium, the theoretical curvature of the kinetoplast DNA fragment is found to be reduced by only a factor of 10%. This value would correspond to about a 20% decrease of RL according to Kop and Crothers (1988). However, a larger decrease of RL is observed. Consequently, unwinding by ditercalinium is not sufficient to explain the dephasing of the dA_n tracts, which causes the kinetoplast curving removal. Other DNA structural modifications must be considered. It must be kept in mind that it has been shown that phasing of dA_n tracts with the helix turn is essential for the gel migration anomaly (Hagerman et al., 1985; Koo et al., 1986; Diekmann, 1986).

Mechanism of DNA Curving Removal. We have observed that a variety of drugs and DNA ligands are able to remove DNA curving. In spite of quite different modes of binding (groove binders and mono- and bisintercalators) and base-pair specificity, these compounds have more or less the same effect on curved DNA. The mechanism by which such ligands remove DNA curving can be discussed only against the background of our understanding of the DNA curving process. Two models have been proposed to account for DNA curving: the wedge model of Trifonov and Sussman (1980) and the junction model, as recently reviewed by Crothers et al. (1990).

In the wedge model, overall curving of DNA is thought to result from the periodic repetition of particular dinucleotides such as AA or TT with a particular roll and tilt. When this occurs, the vectorial summation of roll and tilt along the DNA helix will not cancel out as it does for a random sequence and outright curving will result. Basically, negative rolls in the A-DNA region are not compensated by an opposite roll in the B region.

In the junction model, it is thought that an A tract longer than 4 base pairs adopts a rigid non-B-DNA structure. The basis of this model is the retention of base stacking at the ends of the A tract, causing the adjacent B-DNA helix axes to be directed perpendicular to the plane of inclination of the terminal AT base pairs, which in turn reflects the special structure of the A tracts. The repetition of these local bends in a periodical fashion will cause curving at these positions.

According to the wedge model, a drug could only remove curving by zeroing the vectorial summation of roll and tilt. This could be achieved in several differents ways. AT-specific drugs, like distamycin, would need to induce a positive roll in A tracts to get an overall cancellation of roll. By contrast, GC-specific drugs such as quinomycin or ditercalinium, which bind preferentially to non-A-tract DNA (Mendoza et al., 1990) would need to compensate the DNA alteration present in the A tract. Having opposite effects, the simultaneous binding of both types of drugs is not expected to remove DNA curving. The AT-specific drug will induce a positive roll in the A tract that is canceled by the induced roll from GC-specific drug binding in the B DNA regions. In that case, the vectorial summation of roll will not be canceled out. This has never been observed in spite of the many combinations studied here. In addition, according to this model, each drug is expected to behave quite differently depending on its base pair specificity and its action on roll and tilt.

The junction model permits a better understanding of our results. The anomalous electrophoretic mobility of intrinsically bent DNA fragments in polyacrylamide gel can be explained by considering the reptation model as proposed by Levene and Zimm (1989). It is then easy to understand how a drug that is able to cause a global change in DNA conformation and an increase in DNA flexibility would favor the reptation model. The disorganization of the overall structure of DNA by ligand binding would make local and rigid bends at the junction of A tracts impossible to generate. Drug binding could also modify the flexibility of a DNA chain by straightening a curved fragment due to reversion of dA_n tracts to a more canonical DNA structure. In addition, as discussed above, the smear of DNA bands in gel electrophoresis when partial uncurving is observed implies that the effect of drugs is localized at a very limited number of sites. This is easily understood in the case of the junction model, where bends are supposed to be strictly local. It could not be understood with the wedge model in which DNA curving is per essence delocalized at each dinucleotide.

The ability of DNA–ligand complexes to remove curves in DNA is of biological importance since curved DNA has been found to be associated with the regulation of DNA expression. It is possible that these drugs modify the DNA structure at specific points and thereby prevent DNA looping formation. Such a possibility deserves to be explored.

ACKNOWLEDGMENTS

We thank J. Couprie for her excellent technical help and D. Coulaud for her valuable assistance in the electron microscopy experiments. F.B. is indebted to the French Association de la Recherche sur le Cancer and to Conselleria de Sandidad y Consumo del Gobierno de Baleares (Spain) for financial support. R.M. is grateful for financial assistance from Mexico (CONACYT Grant 43573).

APPENDIX

The following simple model was considered in order to estimate the amount of dye that comigrates with DNA during gel electrophoresis. The gel electrophoresis was estimated to take place in a tube. This tube was divided along its long axis in n elementary slices of equal thickness. To simulate the dissociation and the loss of the dye during electrophoresis, the following algorithm was applied. At the start, the binding ratio r (number of dye molecules bound per nucleotide) was computed from the following equation according to Rêvet et al. (1971)

$$r = \frac{D_t + nP_t + K^{-1} - ((D_t + nP_t + K^{-1})^2 - 4nP_tD_t)^{1/2}}{2P_t} \quad (1)$$

with D_t = total dye concentration, P_t = total DNA concentration expressed in phosphate, n = number of sites per base pair for the dye, and K^{-1} = apparent dissociation constant deduced from a simple Scatchard plot.

When the dye–DNA complex is moved from the slice number i to the slice number $i + 1$, it is assumed that the free dye does not move and is therefore left behind. The total concentration of dye in slice number $i + 1$ is therefore simply the bound concentration of dye in slice number i, that is, r_iP_t.

Introducing this new D_t value in eq 1, the new value of r for slice $i + 1$ is computed and so on.

The decrease of r as a function of K^{-1} and the number of steps can be computed for different initial values.

As an example, we assumed that the DNA concentration was 1×10^{-4} M and the dye concentration was 1×10^{-5} M in the band in the gel, a situation close to our data. A value of 0.2 for n was taken in the calculation. If we consider that the actual thickness of the band is 2 mm, the final situation at the end of electrophoresis will be obtained after 20–40 steps. Therefore, to illustrate the result of such a calculation, we give the relative quantity of dye remaining after 20 and 40 steps for various binding constants.

	no. of steps		
K (M^{-1})	0	20	40
1×10^5	1	0	0
3×10^5	1	0.05	0.002
1×10^6	1	0.27	0.09
3×10^6	1	0.59	0.38
1×10^7	1	0.83	0.71
3×10^7	1	0.98	0.88
1×10^8	1	0.98	0.96

Registry No. **1a** (m = 0), 105823-48-1; **1a** (m = 1), 111159-21-8; **1a** (m = 2), 111159-23-0; **1a** (m = 3), 111159-25-2; **1a** (m = 0, N^7-Me), 133323-99-6; **1b**, 133324-00-2; **1c** (R^2 = Me, R^6 = R^9 = H), 69467-91-0; **1c** (R^2 = R^6 = Me, R^9 = OH), 69467-90-9; **1c** (R^2 = CH_2CH_2Ph, R^6 = H, R^9 = OH), 70173-34-1; poly(dA)·poly(dT), 24939-09-1; poly(dA-dT)·poly(dA-dT), 26966-61-0; ethidium dimer, 61926-22-5; quinomycin C, 11001-74-4; ethidium bromide, 1239-45-8; actinomycin D, 50-76-0; chromomycin A_3, 7059-24-7; distamycin, 39389-47-4; netropsin, 1438-30-8; Hoechst 33258, 23491-45-4.

REFERENCES

Butour, J. L., Delain, E., Coulaud, D., Le Pecq, J. B., Barbet, J., & Roques, B. P. (1978) *Biopolymers 17*, 873–886.
Coll, M., Frederick, C. A., Wang, A. H. J., & Rich, A. (1987) *Proc. Natl. Acad. Sci. U.S.A. 84*, 8385–8389.
Crothers, D. M., Haran, T. E., & Nadeau, J. G. (1990) *J. Biol. Chem. 265*, 7093–7096.
Diekmann, S. (1986) *FEBS Lett. 195*, 53–56.
Fox, K. R., & Waring, M. J. (1984) *Nucleic Acids Res. 12*, 9271–9285.
Fried, M. G., & Crothers, D. M. (1981) *Nucleic Acids Res. 13*, 6505–6525.
Garbay-Jaureguiberry, C., Laugaa, P., Delepierre, M., Laalami, S., Muzard, G., Le Pecq, J. B., & Roques, B. P. (1987) *Anti-Cancer Drug Des. 1*, 323–335.
Gaugain, B., Barbet, J., Capelle, N., Roques, B. P., & Le Pecq, J. B. (1978) *Biochemistry 17*, 5078–5088.
Glazer, A. N., Peck, K., & Mathies, R. A. (1990) *Proc. Natl. Acad. Sci. U.S.A. 87*, 3851–3855.
Griffith, J., Bleyman, M., Rauch, C. A., Kitchin, P. A., & Englund, P. T. (1986) *Cell 46*, 717–724.
Hagerman, P. J. (1985) *Biochemistry 24*, 7033–7037.
Haran, T. E., & Crothers, D. M. (1988) *Biochemistry 27*, 6967–6971.
Hartley, J. L., & Gregori, T. J. (1981) *Gene 13*, 347–353.
Joanicot, M., & Rêvet, B. (1987) *Biopolymers 26*, 315–326.
Keller, W. (1975) *Proc. Natl. Acad. Sci. U.S.A. 72*, 4876.
Kitchin, P. A., Klein, V. A., Ryan, K. A., Gann, K. L., Rauch, C. A., Kang, D. S., Wells, R. D., & Englund, P. T. (1986) *J. Biol. Chem. 261*, 11302–11309.
Koo, H. S., & Crothers, D. M. (1988) *Proc. Natl. Acad. Sci. U.S.A. 85*, 1763–1767.
Koo, H. S., Wu, H. M. & Crothers, D. M. (1986) *Nature 320*, 501–506.
Kopka, M. L., Yoon, C., Goodsell, D., Pjura, P., & Dickerson, R. E. (1985) *Proc. Natl. Acad. Sci. U.S.A. 82*, 1376–1380.
Levene, S. D., & Zimm, B. H. (1989) *Science 245*, 396–399.
Maniatis, T., Fritsch, E. F., & Sambrook, J. (1982) *Molecular Cloning: A Laboratory Manual*, Cold Spring Harbor Laboratory, Cold Spring Harbor, NY.
Marini, J. C., Levene, S. D., Crothers, D. M., & Englund, P. T. (1982) *Proc. Natl. Acad. Sci. U.S.A. 79*, 7664–7668.
McGhee, J. D., & Von Hippel, P. H. (1974) *J. Mol. Biol. 86*, 469–489.
Mendoza, R., Markovits, J., Muzard, G., & Le Pecq, J. B. (1990) *Biochemistry 29*, 5035–5043.
Muller, W., & Crothers, D. M. (1968) *J. Mol. Biol. 35*, 251–290.
Muzard, G., Thêveny, B., & Rêvet, B. (1990) *EMBO J. 9*, 1289–1298.
Nielsen, P. E., Zhen, W., Henriksen, U., & Buchardt, O. (1988) *Biochemistry 27*, 67–73.
Pelaprat, D., Delbarre, A., Le Guern, I., & Roques, B. P. (1980) *J. Med. Chem. 23*, 1336–1343.
Qi Gao, Williams, L. D., Egli, M., Rabinovich, D., Chen, S.-L., Quigley, G. J., & Rich, A. (1991) *Proc. Natl. Acad. Sci. U.S.A.* (in press).
Rêvet, B. M. J., Schmir, M., & Vinograd, J. (1971) *Nature, New Biol. 229*, 10–13.
Rice, J. A., Crothers, D. M., Pinto, A. L., & Lippard, S. J. (1988) *Proc. Natl. Acad. Sci. U.S.A. 85*, 4158–4161.
Roques, B. P., Barbet, J., Oberlin, R., & Le Pecq, J. B. (1976) *C. R. Acad. Sci. Paris, Ser. D 283*, 1365–1368.

Schleif, R. (1988) *Science 240*, 127-128.
Sinden, R. R., & Hagerman, P. J. (1984) *Biochemistry 23*, 6299-6303.
Stellwagen, N. C. (1983) *Biochemistry 22*, 6186-6193.
Thêveny, B., Coulaud, D., Le Bret, M., & Rêvet, B. (1988) in *Structure and Expression Vol. 3: DNA Bending & Curvature*, pp 39-55, Adenine Press, Guilderland, NY.
Trifonov, E. N., & Sussman, J. L. (1980) *Proc. Natl. Acad. Sci. U.S.A. 77*, 3816-3820.
Trifonov, E. N., & Ulanovsky, L. E. (1988) in *Unusual DNA Structures* (Wells, R. D., & Harvey, S. C., Eds.) Springer-Verlag, New York.
Van Dyke, M. W., Hertzberg, R. P., & Dervan, P. B. (1982) *Proc. Natl. Acad. Sci. U.S.A. 79*, 5470-5474.
Van Dyke, M. W., & Dervan, P. B. (1983) *Biochemistry 22*, 2373-2377.
Van Dyke, M. M., & Dervan, P. B. (1984) *Science 225*, 1122-1127.
Wang, J. C., & Giaever, G. N. (1988) *Nature 240*, 300-304.
Wakelin, L. P. G. (1986) *Med. Res. Rev. 6*, 275-340.
Waring, M. J. (1981) *Annu. Rev. Biochem. 50*, 159-192.
Wu, H. M., & Crothers, D. M. (1984) *Nature 308*, 509-513.
Zimmer, C., & Wahnert, U. (1986) *Prog. Biophys. Mol. Biol. 47*, 31-112.

Chemical Nature of DNA-Protein Cross-Links Produced in Mammalian Chromatin by Hydrogen Peroxide in the Presence of Iron or Copper Ions†

Zeena Nackerdien,‡,§ Govind Rao,‖ Marco A. Cacciuttolo,‖ Ewa Gajewski,‡ and Miral Dizdaroglu*,‡

Chemical Science & Technology Laboratory, National Institute of Standards and Technology, Gaithersburg, Maryland 20899, Department of Radiotherapy, University of Stellenbosch, Tygerberg, South Africa, and Chemical and Biochemical Engineering, University of Maryland Baltimore County, and Medical Biotechnology Center, Maryland Biotechnology Institute, Baltimore, Maryland 21228

Received January 2, 1991

ABSTRACT: We report on the elucidation of DNA-protein cross-links formed in isolated mammalian chromatin upon treatment with H_2O_2 in the presence of iron or copper ions. Analysis of chromatin samples by gas chromatography/mass spectrometry after hydrolysis and derivatization showed the presence of 3-[(1,3-dihydro-2,4-dioxopyrimidin-5-yl)methyl]-L-tyrosine (thymine-tyrosine cross-link) on the basis of the gas chromatographic and mass spectrometric characteristics of the trimethylsilylated authentic compound. Other DNA-protein cross-links involving thymine and the aliphatic amino acids and cytosine and tyrosine, which were known to occur in nucleohistone γ-irradiated under anoxic conditions, were not observed. This was due to inhibition by oxygen as clearly shown by experiments that were carried out using ionizing radiation under both oxic and anoxic conditions instead of using H_2O_2 and metal ions. However, oxygen did not inhibit formation of the thymine-tyrosine cross-link in γ-irradiated chromatin or in chromatin treated with H_2O_2 and metal ions. The yield of the thymine-tyrosine cross-link was higher upon treatment with H_2O_2/chelated Fe^{3+} ions than with H_2O_2/unchelated Fe^{3+} ions. By contrast, H_2O_2/unchelated Cu^{2+} ions produced a higher yield than H_2O_2/chelated Cu^{2+} ions. Almost complete inhibition of cross-link formation was provided by the hydroxyl radical scavengers mannitol and dimethyl sulfoxide when H_2O_2/chelated metal ions were used. On the other hand, scavengers only partially inhibited formation of cross-links when H_2O_2/unchelated metal ions were used, possibly indicating the site-specific nature of cross-linking. Superoxide dismutase afforded partial inhibition only when chelated ions were used. The mechanism underlying formation of this DNA-protein cross-link is thought to involve addition of the hydroxyl radical generated allyl radical of thymine to carbon-3 of tyrosine followed by subsequent oxidation of the adduct radical.

Free radicals produced in vivo have been implicated in the occurrence of a number of biological processes including mutagenesis and carcinogenesis [for a review see Halliwell and Gutteridge (1989)]. Excess generation of free radicals in living cells by endogenous or exogenous sources may result in damage to biological molecules including DNA. Oxygen-derived species such as superoxide radical (O_2^-)[1] and H_2O_2 are generated in mammalian cells as a result of aerobic metabolism and also by exogenous sources such as redox-cycling drugs [for reviews see Halliwell and Gutteridge (1989) and Fridovich (1986)]. However, neither O_2^- nor H_2O_2 appears to produce strand breaks in DNA or to cause modification of bases in DNA (Lesko et al., 1980; Rowley & Halliwell, 1983; Sagripanti & Kraemer, 1989; Aruoma et al., 1989a,b; Blakely et al., 1990). Thus much of the toxicity of O_2^- and H_2O_2 in vivo is thought to arise from their metal ion dependent conversion into hydroxyl radical (•OH) (Halliwell & Gutteridge, 1989, 1988; Mello-Filho & Meneghini, 1985; Nassi-Calo et al.,

† This work was supported in part by the Office of Health and Environmental Research, Office of Energy Research, U.S. Department of Energy, Washington, DC. Z.N. acknowledges support from the South African Medical Reserach Council. G.R. acknowledges support from the National Science Foundation, Washington, DC, Grant EE-8808775.
* To whom correspondence should be addressed.
‡ National Institute of Standards and Technology.
§ University of Stellenbosch.
‖ University of Maryland Baltimore County and Maryland Biotechnology Institute.

[1] Abbreviations: O_2^-, superoxide radical; •OH, hydroxyl radical; DPC, DNA-protein cross-link; NTA, nitrilotriacetic acid; SOD, copper-zinc superoxide dismutase; Phe-Phe, phenylalanylphenylalanine; asc, ascorbic acid; BSTFA, bis(trimethylsilyl)trifluoroacetamide; GC/MS-SIM, gas chromatography/mass spectrometry with selected-ion monitoring; Thy, thymine; Cyt, cytosine; Thy-Tyr cross-link, 3-[1,3-dihydro-2,4-dioxopyrimidin-5-yl)methyl]-L-tyrosine; chr, chromatin; Gy, gray (J/kg).

0006-2960/91/0430-4873$02.50/0